Modulation of Glucose Production by Central Insulin Requires IGF-1 Receptors in AgRP Neurons

Gabriela Farias Quipildor,[1,2,3] Kai Mao,[1,2,3] Pedro J. Beltran,[4] Nir Barzilai,[2,3,5,6] and Derek M. Huffman[1,2,3,5]

Diabetes 2021;70:2236–2248 | https://doi.org/10.2337/db21-0028

Similar to insulin, central administration of IGF-1 can suppress hepatic glucose production (HGP), but it is unclear whether this effect is mediated via insulin receptors (InsRs) or IGF-1 receptors (IGF-1Rs) in the brain. To this end, we used pharmacologic and genetic approaches in combination with hyperinsulinemic-euglycemic clamps to decipher the role of these receptors in mediating central effects of IGF-1 and insulin on HGP. In rats, we observed that intracerebroventricular (ICV) administration of IGF-1 or insulin markedly increased the glucose infusion rate (GIR) by >50% and suppressed HGP ($P < 0.001$). However, these effects were completely prevented by preemptive ICV infusion with an IGF-1R and InsR/IGF-1R hybrid (HybridR) blocking antibody. Likewise, ICV infusion of the InsR antagonist, S961, which also can bind HybridRs, interfered with the ability of central insulin, but not IGF-1, to increase the GIR. Furthermore, hyperinsulinemic clamps in mice lacking IGF-1Rs in AgRP neurons revealed ~30% reduction in the GIR in knockout animals, which was explained by an impaired ability of peripheral insulin to completely suppress HGP ($P < 0.05$). Signaling studies further revealed an impaired ability of peripheral insulin to trigger ribosomal S6 phosphorylation or phosphatidylinositol (3,4,5)-trisphosphate production in AgRP neurons lacking IGF-1Rs. In summary, these data suggest that attenuation of IGF-1R signaling in the mediobasal hypothalamus, and specifically in AgRP neurons, can phenocopy impaired regulation of HGP as previously demonstrated in mice lacking InsRs in these cells, suggesting a previously unappreciated role for IGF-1Rs and/or HybridRs in the regulation of central insulin/IGF-1 signaling in glucose metabolism.

Insulin has previously been established as an important central regulator of peripheral metabolism (1–8). Obici et al. (2) initially showed that central delivery of insulin directly suppressed hepatic glucose production (HGP) during insulin clamp studies in rats. Several subsequent reports using strategies to disrupt insulin signaling in the brain or periphery have confirmed that central insulin action is critical to maintaining glucose homeostasis (6,9). Furthermore, studies using genetic or pharmacologic strategies to disrupt insulin receptors (InsRs) strongly support that InsR signaling is required for mediating the effects of central insulin (1,2,7,8). Moreover, Könner et al. (8) was able to demonstrate that insulin action at the level of hypothalamic AgRP-expressing neurons is required for suppression of glucose production by the liver. Similarly, chronic reduction of InsRs in the ventromedial hypothalamus has been shown to lead to glucose intolerance in nonobese nondiabetic rats (10).

IGF-1, which is a hormone closely related to insulin, is most well-known for its role in somatic growth and development (11). However, IGF-1 has also been shown to have insulin-like effects on glucose metabolism, including the promotion of glucose uptake and suppression of HGP, while serum IGF-1 levels have been inversely related to type 2 diabetes risk in some epidemiological studies (12–14). IGF-1 primarily signals via IGF-1 receptors (IGF-1Rs) or InsR/IGF-1R hybrids (HybridRs). However,

[1]Department of Molecular Pharmacology, Albert Einstein College of Medicine, Bronx, NY
[2]Institute for Aging Research, Albert Einstein College of Medicine, Bronx, NY
[3]Fleischer Institute for Diabetes & Metabolism, Albert Einstein College of Medicine, Bronx, NY
[4]Oncology Research, Amgen Inc., Thousand Oaks, CA
[5]Department of Medicine, Albert Einstein College of Medicine, Bronx, NY
[6]Department of Genetics, Albert Einstein College of Medicine, Bronx, NY
Corresponding author: Derek M. Huffman, derek.huffman@einsteinmed.org

Received 11 January 2021 and accepted 16 July 2021
This article contains supplementary material online at https://doi.org/10.2337/figshare.14997825.
G.F.Q. and K.M. contributed equally.

IGF-1Rs are only scantly expressed on hepatocytes, suggesting that IGF-1 may suppress HGP through other sites, such as the brain. Indeed, it was demonstrated that central delivery of IGF-1 during an insulin clamp markedly suppressed HGP in rats (15), reminiscent of effects with intracerebroventricular (ICV) insulin.

Although central insulin and IGF-1 similarly suppress HGP, the mechanism(s) whereby IGF-1 acts centrally, and rather these effects occur via a distinct or overlapping manner, remains elusive. IGF-1 may mediate these effects via binding IGF-1Rs to trigger shared downstream effectors as InsR signaling. Alternatively, IGF-1 can bind the InsR, albeit with much lower affinity than the IGF-1R (16), and may act to suppress HGP via this canonical pathway. However, IGF-1 and insulin have exquisite affinity for their respective receptors, and the complexity of how these ligands might impact cell signaling is further complicated by evidence that both IGF-1 and insulin can elicit distinct cellular responses due to unique interactions between ligand and receptor and distinct properties inherent to each cognate receptor (17,18).

Thus, in order to better understand the receptor(s) mediating the effects of central IGF-1 to suppress HGP, we have used pharmacologic and genetic strategies in combination with in vivo studies. Here we show that interfering with IGF-1R signaling, either by pharmacologic blockade or genetic disruption of IGF-1Rs specifically in AgRP neurons, is sufficient to block the ability of central IGF-1 to modulate peripheral insulin action and suppress HGP. Remarkably, attenuating IGF-1R signaling was also sufficient to attenuate the ability of insulin to regulate peripheral metabolism or to activate insulin signaling pathways in AgRP neurons, suggesting that intact InsRs alone in AgRP neurons are not sufficient to mediate the effects of insulin. Instead, these data suggest that activation of this pathway may require cooperative effects of InsRs, IGF-1Rs, and potentially HybridRs, which are highly expressed in brain and are particularly abundant in neurons. Indeed, removal of HybridRs would be a common feature to both InsR and IGF-1R deletion or inhibition, suggesting a potentially important and previously unappreciated role for these receptors in the regulation of glucose homeostasis.

RESEARCH DESIGN AND METHODS

Animals

Young (3-month-old) male Fisher × Brown Norway (FBN) F1 hybrid rats were obtained from the National Institute on Aging aged rodent colony. Rats were individually housed and allowed to acclimate for at least 1 week upon arrival before undergoing any surgical procedures. For the generation of knockout (KO) mice, *Igf1r*$^{flox/flox}$ mice (stock no. 012251) and *Agrp-IRES-Cre* mice (012899) were obtained from The Jackson Laboratory (Bar Harbor, MA) and *Igf1r*$^{flox/flox}$*–Agrp-IRES-Cre*$^{+/-}$ were mated with *Igf1r*$^{flox/flox}$ mice to produce *Igf1r*$^{\Delta AgRP}$ (referred to hereafter as KO) and *Igf1r*$^{flox/flox}$ (control) offspring. For immunostaining and single-cell studies, *Igf1r*$^{flox/flox}$ mice were mated with *Agrp-IRES-Cre* and *NPY-GFP* [B6.FVB-Tg(Npy-hrGFP)1Lowl/J, stock no. 006417; The Jackson Laboratory] mice to generate KO and control animals with GFP-expressing NPY/AgRP neurons for either peripheral saline or insulin treatment. Mice were housed either individually for longitudinal measures or group housed for other experiments. All animals were kept at standard temperature (~22°C) and humidity-controlled conditions under a 14 hours light–10 hours dark photoperiod and provided ad libitum access to water and chow. All experiments were approved by the Institutional Animal Care and Use Committee at the Albert Einstein College of Medicine.

Surgeries

All surgical procedures were conducted under 2% isoflurane. Stereotactic placement of a steel guide cannula (PlasticsOne, Roanoke, VA) reaching the 3rd ventricle was performed in rats (coordinates from bregma: 0.2 mm anterior/posterior, −9.0 mm dorsal/ventral, 0.0 directly on the midsagittal suture), and the implant was secured in place with dental cement and treated with analgesic for up to 3 days. Approximately 14 days later, animals were either used for experiments or sedated a second time for surgical placement of indwelling catheters into the right internal jugular vein and the left carotid artery as previously described (19–21). Likewise, mice used for clamp studies underwent similar placement of vascular catheters under isoflurane anesthesia and supportive care was provided. Recovery was monitored until animals were within 3% of their preoperative weight (5–7 days) before subsequent clamp studies were conducted.

Hyperinsulinemic-Euglycemic Clamp Studies in Rats

We performed hyperinsulinemic-euglycemic clamp studies with ICV infusion of peptides and/or inhibitors, respectively, to evaluate central regulation of insulin sensitivity, similar to studies previously described (19,20). All studies were 360 min in duration and consisted of a 120-min equilibration period, 120-min basal period, and 120-min hyperinsulinemic clamp period. Beginning at $t = -15$ min, animals received a primed continuous ICV infusion of artificial cerebral spinal fluid (aCSF); an IGF-1R (and HybridR) antagonist (IGF-1R monoclonal antibody [mAb], Amgen Inc.) (22), provided as a 12-μg bolus over 15 min, followed by a continuous infusion of 18 μg over 6 h (3 $\mu g \cdot h^{-1}$; 30 μg total dose); or the InsR (and HybridR) small peptide inhibitor, S961 (Novo Nordisk) (23), provided as a 240-pmol bolus over 15 min, followed by a continuous infusion of 400 pmol over 6 h (66 $pmol \cdot h^{-1}$; 640 pmol total dose). At $t = 0$ min, animals were provided a second primed continuous ICV infusion of aCSF; 1 μg human IGF-1, provided as a 0.3-μg bolus over 7.5

min, followed by a continuous infusion of 0.7 μg over 6 h (0.12 $\mu g \cdot h^{-1}$); or 30 μU insulin, provided first as a bolus of 7.5 μU over 7.5 min and then as a continuous infusion of 22.5 μU over 6 h (3.8 $\mu U \cdot h^{-1}$) as previously described (19).

At $t = 120$ min, which is the beginning of the basal period, a primed continuous infusion of [3-^{3}H]-glucose (20 μCi bolus, 0.2 μCi/min maintenance; NEN Life Science Products, Boston, MA) was given into the jugular vein and maintained throughout the remainder of the study. The hyperinsulinemic-euglycemic clamp was then initiated at $t = 240$ min by peripheral administration of a primed continuous infusion of regular insulin (3 $mU \cdot kg^{-1} \cdot min^{-1}$), and somatostatin (1.5 $\mu g \cdot kg^{-1} \cdot min^{-1}$) was also provided to suppress endogenous insulin secretion. A 25% glucose solution was given and periodically adjusted to clamp the plasma glucose concentration at ~140–145mg/dL. Serum samples for determination of [3-^{3}H]-glucose and [3-^{3}H]-glucose water specific activities were obtained at 10-min intervals during the basal and clamp periods. At the completion of the study, rats were killed with a lethal dose of intravenous pentobarbital sodium (100 mg/kg body wt). Several tissues were then rapidly excised, weighed, and flash frozen in liquid nitrogen, prior to storage at −80°C.

Body Weight and Food Intake in Mice

For determination of possible effects of IGF-1Rs in AgRP neurons on energy balance, KO ($n = 12$) and control ($n = 13$) male mice as well as KO ($n = 12$) and control ($n = 11$) female mice were singly housed at weaning and body weight and food intake were monitored and recorded until 16 weeks of age.

Glucose, Insulin, and Pyruvate Tolerance Tests in Mice

Glucose metabolism and insulin sensitivity were assessed in KO ($n = 13$) and control ($n = 10$) male mice. Glucose tolerance tests (GTTs) and insulin tolerance tests (ITTs) were performed essentially as previously described (24,25). Briefly, at 12–14 weeks of age, mice were fasted for 4 h, a baseline blood glucose measurement was taken, and animals were injected with 2 mg/kg glucose i.p., and blood glucose was measured at 15, 30, 60, 90, and 120 min postinjection with a glucose meter (CONTOUR; Bayer). ITTs were performed ~1 week later in random-fed mice early in their light cycle (~0700–0800 h) as previously described (24). Briefly, following a baseline glucose measurement, mice were injected with 1 unit/kg i.p. insulin and blood glucose was measured at 15, 30, 45, and 60 min later. For the pyruvate tolerance test (PTT), mice were fasted overnight. Following a baseline glucose measurement, mice were then injected with pyruvate at a dose of 2 g/kg, and glucose levels were monitored at 15, 30, 60, 90, and 120 min (26).

Hyperinsulinemic-Euglycemic Clamp Studies in Mice

We performed hyperinsulinemic-euglycemic clamp studies in conscious, unrestrained, catheterized KO ($n = 10$) and control male mice ($n = 10$) similar to studies previously described (27,28). All studies were 240 min in duration. The protocol consisted of a 120-min tracer equilibration basal period, first with infusion of [3-^{3}H]-glucose (5 μCi bolus, 0.05 μCi/min maintenance). A continuous infusion of insulin (1.5 $mU \cdot kg^{-1} \cdot min^{-1}$) was then initiated and [3-^{3}H]-glucose was increased to 0.1 μCi/min for the remaining 2 h of the clamp. Food was removed from the hopper ~3 h prior to initiation of the clamp, and we collected plasma samples to determine glucose levels at baseline, prior to initiating exogenous insulin, and glucose level was monitored every 10 min thereafter to 120 min. Additional blood was collected at 90–120 min for measuring insulin level and [3-^{3}H]-glucose and [3-^{3}H]-glucose water specific activities. The total volume of blood withdrawn was ~250 μL/study. Volume depletion and anemia were prevented by resuspending of washed red blood cells in 10 units/mL heparinized saline and infusion back into the animal. At the end of the clamp study, animals were killed by exsanguination and tissues were rapidly excised, weighed, and flash frozen in liquid nitrogen, prior to storage at −80°C.

Assays and Analytical Procedures

Serum glucose was monitored throughout the clamp via the glucose oxidase method with an Analox GM7 analyzer (Analox Instruments USA, Lunenberg, MA) for rats and via glucose test strips in mice. Endogenous insulin was measured with a rat/mouse ELISA (EMD Millipore) with rat insulin standards, and clamp insulin levels were measured with a human ELISA (ALPCO, Salem, NH) with human insulin standards.

Calculations of Whole-Body Glucose Fluxes

Estimation of glucose fluxes during the clamp were carried out as previously described (19–21,29). Briefly, [3-^{3}H]-glucose radioactivity was measured in duplicates in the supernatants of $Ba(OH)_2$ and $ZnSO_4$ precipitates of serum samples (10 μL in mice, 50 μL in rats) after evaporation to dryness to eliminate tritiated water. Under steady-state conditions for plasma glucose concentrations, the glucose R_d equals the R_a. The R_a was calculated as the ratio of the rate of infusion of [3-^{3}H]-glucose (disintegrations per minute) and the steady-state serum [3-^{3}H]-glucose specific activity (disintegrations per minute per milligram). The rate of HGP was calculated as the difference between R_a and the glucose infusion rate (GIR). The rates of glycolysis and glycogen synthesis were estimated as previously described (15).

In Vitro Studies

The SH-SY5Y human neuroblastoma cell line, obtained from ATCC (CRL-2266), and the adult hypothalamic mHypoA-NPY/GFP cell line (CLU499; Cedarlane) were

cultured in DMEM with 10% FBS. On reaching 80–90% confluence, cells were serum starved for 4 h prior to the experiment. For demonstration of in vitro specificity of inhibitors, cells were pretreated with vehicle, S961 (100 ng/mL), or IGF-1R mAb (100 μg/mL) diluted in serum-free media. One hour later, each pretreatment condition was subsequently challenged with vehicle, IGF-1 (10 nmol/L), or insulin (10 nmol/L) in duplicate, and cells were collected and lysed on ice with radioimmunoprecipitation assay buffer 30 min after challenge for analysis of downstream insulin/IGF-1 signaling markers, as described below.

RNA Isolation and Expression

Total RNA from frozen tissues was isolated with use of the Trizol procedure as previously described. First-strand cDNA was synthesized with random primers and total RNA as a template using iScript cDNA Synthesis Kit (Bio-Rad Laboratories, Hercules, CA). InsR-A and B isoform expression in multiple tissues was performed as previously described (30). Following PCR with primers designed to amplify both InsR isoforms, products were resolved on a 4% agarose gel (Life Technologies). Gene expression in single-cell samples was performed for *IGF-1R* (forward, 5′-GCAGTAGGCACCCTTGGTAA, and reverse, 5′-AAATGCCCACAGTTCACT), *InsR* (forward 5′-TCAAGACCAGACCCGAAGATT, and reverse, 5′-TCTCGAAGATAACCAGGGCATAG), *NPY* (forward, 5′-ATGCTAGGTAACAAGCGAATGG, and reverse, 5′-TGTCGCAGAGCGGAGTAGTAT), and *18S* (forward, 5′-TTGACGGAAGGGCACCACCAG, and reverse, 5′-GCACCACCACCCACGGAATCG). For gene expression in rat liver, the following primers were used: *IL-6* (forward, 5′-GTGGCTAAGGACCAAGACCA, and reverse, CATTCATATTGCCAGTTCTTCG), *Gsk3b* (forward, 5′-ATTACGGGACCCAAATGTCA, and reverse, CCACGGTCTCCAGCATTAGT), *Gck* (forward, 5′-AGACCAGACCCCAGGAGAGT, and reverse, GGTCCCCTTAGAGCAAGGAC), *Pc* (forward, 5′-AGATGCACTTCCATCCCAAG, and reverse, CCTTGGTCACGTGAACCTTT), *Pepck* (forward, 5′-CCCCAGGAAGTGAGGAAG, and reverse, GACCGTCTTGCTTTCGATCC), *G6pase* (forward, 5′-ACCCTGGTAGCCCTGTCTTT, and reverse, GGGCTTTCTCTTCTGTGTCG), and *Pygl* (forward, 5′-GTGAACACTATGCGCCTCTG, and reverse, CCTCAGCTCCTTCCCTTCAA), and data were normalized to *Ppia* (forward, 5′-AGCACTGGGGAGAAAGGATT, and reverse, AGCCACTCAGTCTTGGCAGT) using the ΔΔCt method.

Protein Isolation and Western Blot

Total protein from cells and tissues was extracted with radioimmunoprecipitation assay buffer, and total protein content was determined with the BCA protein assay (Sigma-Aldrich, St. Louis, MO) with BSA as a standard. Proteins were separated by SDS-PAGE with Bis-Tris gels (Bio-Rad Laboratories), transferred onto polyvinylidene fluoride membranes at 100 V constant for 1 h, and incubated with an appropriate primary antibody against phosphorylated (p)Akt^{Thr308} (13038; Cell Signaling Technology), pAkt^{Ser473} (4060; Cell Signaling Technology), total Akt (4691; Cell Signaling Technology), p-p44/42MAPK$^{Thr202/Tyr204}$ (9101; Cell Signaling Technology), and total p44/42 MAPK (9107; Cell Signaling Technology) IGF-1R (9750; Cell Signaling Technology) or InsRβ (9H4; Santa Cruz Biotechnology) overnight at 4°C (24,31). Following a 1-h incubation with secondary antibody, Clarity Western ECL Substrate (Bio-Rad Laboratories) was applied to the membrane and bands were visualized with a ChemiDoc bio-imager (Bio-Rad Laboratories) to first pixel saturation and densitometry performed with Image Lab (Bio-Rad Laboratories).

Hypothalamic Slice Preparations and Single-Cell Quantitative PCR

Coronal slices were obtained from 3-month-old *NPY/GFP* reporter mice ($n = 4$). In brief, animals were decapitated and their brains were transferred into an ice-cold sucrose-based solution bubbled with 95% O_2 and 5% CO_2 as previously described (32). A vibratome was used to prepare 200-μm coronal slices, which were kept in oxygenated aCSF solution at 37°C. An upright, infrared-differential interference contrast microscope (Olympus BX50WI) mounted on a Gibraltar X-Y table (Burleigh) was used to visualize NPY/AgRP fluorescent cells in hypothalamic brain sections at a 40× magnification. With aspiration into a patch glass pipette, cytoplasm containing total RNA was collected from individual single NPY/AgRP neurons. Then, each cell was placed into a 0.2-mL microcentrifuge tube by pressure ejection and further processed for reverse transcription to cDNA with a REPLI-g WTA Single Cell Kit (QIAGEN) per the manufacturer's guidelines. A column-based MEGAquick-spin Plus Total Fragment DNA Purification Kit (cat. no. 17287; iNtRON Biotechnology) was used to purify the cDNA, and its concentration was measured with a NanoDrop ND-1000 spectrophotometer (Thermo Fisher Scientific). Single-cell quantitative PCR was performed as described above, and PCR products were run on a 2% agarose gel to verify product size. InsR and IGF-1R products were subsequently sent for sequencing to the Einstein Genomics Core for confirmation of the final product.

In Vivo Receptor Distribution and Immunoprecipitation for Hybrid Receptor Levels

For determination of relative InsR and IGF-1R levels, standard Western blotting was performed, while HybridR content in tissues was assessed by immunoprecipitation as previously described (24). In brief, 70 μg total protein was immunoprecipitated from several rat tissues ($n = 4$ each) with 1 μg anti–IGF-1R antibody (9750; Cell Signaling Technology) overnight, using the Catch and Release v2.0 Reversible Immunoprecipitation System (EMD Millipore) as previously described (24). Equal volumes of eluted sample containing immunoprecipitated protein were then loaded and separated by SDS-PAGE, transferred onto polyvinylidene fluoride

membranes, probed with anti-InsRβ antibody (C-19; Santa Cruz Biotechnology), and visualized as described above.

In Vivo Activation Studies

For determination of the relative abilities of insulin and IGF-1 to trigger shared downstream signaling mediators in mediobasal hypothalamus (MBH), FBN rats were implanted with an ICV catheter and, ∼14 days later, were assigned to receive an ICV infusion of aCSF, IGF-1 (1 μg), or an equimolar dose of insulin (22 mU) over 5 min. For evaluation of downstream signaling of pAkt, animals were euthanized at 15 min after initiation of infusion and MBH wedges were collected as previously described for Western blotting (19,33). For evaluating insulin signaling specifically in AgRP neurons, a jugular catheter was inserted into *Igf1r*$^{flox/flox}$ (control) and *Igf1r*$^{\Delta AgRP}$*–NPY-GFP* (KO) reporter mice. One week later, animals were fasted overnight, infused with an intravenous dose of insulin (0.2 units/min over 5 min; 1 unit total dose) or saline, and then sedated and transcardially perfused 10 min later. Brain tissue was then rapidly excised for further processing.

Immunohistochemistry

For immunostaining in brain tissue, animals were transcardially perfused with room temperature 0.1 mol/L PBS (pH 7.4) followed by ice-cold 4% paraformaldehyde in PBS. Brains were removed, postfixed overnight at 4°C, and then infiltrated with 30% sucrose in 0.1 mol/L PBS at 4°C and frozen. Serial coronal sections of 30 μm thickness were cut at 160-μm intervals on a cryostat (Leica CM1950; Leica, Wetzlar, Germany) and collected in PBS with 1% sodium azide until processing. For 3,3′-diaminobenzidine (DAB) detection, free-floating sections were incubated in 3% hydrogen peroxide in 0.1 mol/L PBS for 30 min, rinsed, and incubated in 0.5% Triton X-100 in 0.1 mol/L PBS with 10% normal goat serum for 1 h at room temperature and then incubated overnight at 4°C in rabbit pAkt^{Ser473}(4060; Cell Signaling Technology). Sections were incubated in biotinylated goat anti-rabbit IgG (1:300, BA-1000; Vector Laboratories, Burlingame, CA) for 2 h, rinsed, and incubated in avidin-biotin complex (VECTASTAIN Elite; Vector Laboratories) for 90 min prior to DAB exposure (DAB Substrate Kit; Vector Laboratories). Imaging was conducted with the PANORAMIC 250 Flash II Slide Scanner (3DHISTECH).

Immunofluorescence was performed for pS6 activation and phosphatidylinositol (3,4,5)-trisphosphate (PIP_3) formation in AgRP neurons in response to insulin. Specifically, rabbit monoclonal pS6$^{Ser240/Ser242}$ (cat. no. 5364; Cell Signaling Technology) and mouse monoclonal PIP_3 (z-P345; Echelon Biosciences) were used as primary antibodies. A mouse-on-mouse (M.O.M). immunodetection kit was used for PIP_3 staining (BMK-2202; Vector Laboratories) in order to block endogenous mouse IgG staining. Free-floating sections were then incubated in either goat anti-rabbit Alexa Fluor 568 (A-11036; Thermo Fisher Scientific) or goat anti-mouse Alexa Fluor 565 (A-11004; Thermo Fish Scientific) for 90 min, rinsed, and mounted with mounting medium with DAPI (VECTASHIELD, cat. no. H-1200; Vector Laboratories). Immunofluorescent images were taken with a Leica SP5 confocal microscope with a 63× magnification and with a zoom value of 2. For pS6 immunofluorescence, images were analyzed with measurement of the mean fluorescence intensity within NPY cells using the Volocity 6.3 software (PerkinElmer); PIP_3 immunofluorescence was analyzed in ImageJ, using deconvolution analysis, and the JACoP plugin was used for colocalization coefficient analysis.

Statistics

Longitudinal measures were assessed by repeated-measures ANOVA and cross-sectional measures were assessed by one-way ANOVA. When a significant effect was observed, planned contrasts with Tukey honestly significant difference or Dunnett adjustment, when appropriate, were applied to determine individual differences among groups. All analyses were performed with SPSS (SPSS, Chicago, IL). All values are presented as means ± SE. A $P \leq 0.05$ was considered statistically significant.

Data and Resource Availability

Data generated and/or analyzed in the current study are available from the corresponding authors on reasonable request.

RESULTS

IGF-1Rs, InsRs, and HybridRs are Abundantly Expressed in the MBH

To investigate the relative distribution of InsRs, IGF-1Rs, and HybridRs among tissue types, we measured protein expression in several central and peripheral tissues. InsRs were detected to various degrees in all analyzed tissues but were relatively most abundant in liver, pancreas, and MBH (Fig. 1*A*). However, IGF-1Rs and HybridRs were mainly enriched in brain tissues, whereas levels in many peripheral organs were lowly expressed or even below the level of detection as a function of total protein loaded (Fig. 1*B* and *C*). Similar to previous reports, in assessment of the presence of InsR isoforms A and B among tissues, while liver mainly fexpresses InsR isoform B, InsR-A was the most abundantly present isoform in brain tissues, including MBH, whereas adipose and skeletal muscle expressed both InsR-A and -B (Fig. 1*D*). Moreover, consistent with the abundant expression of IGF-1Rs in MBH, an acute ICV IGF-1 injection was able to stimulate downstream signaling in the arcuate nucleus, as demonstrated by an increase in pAkt^{Ser473} and pAkt^{Thr308} (Fig. 1*E* and *F*) ($P < 0.05$), whereas insulin led to more variable Akt activation that was not significant after Tukey adjustment, but significantly

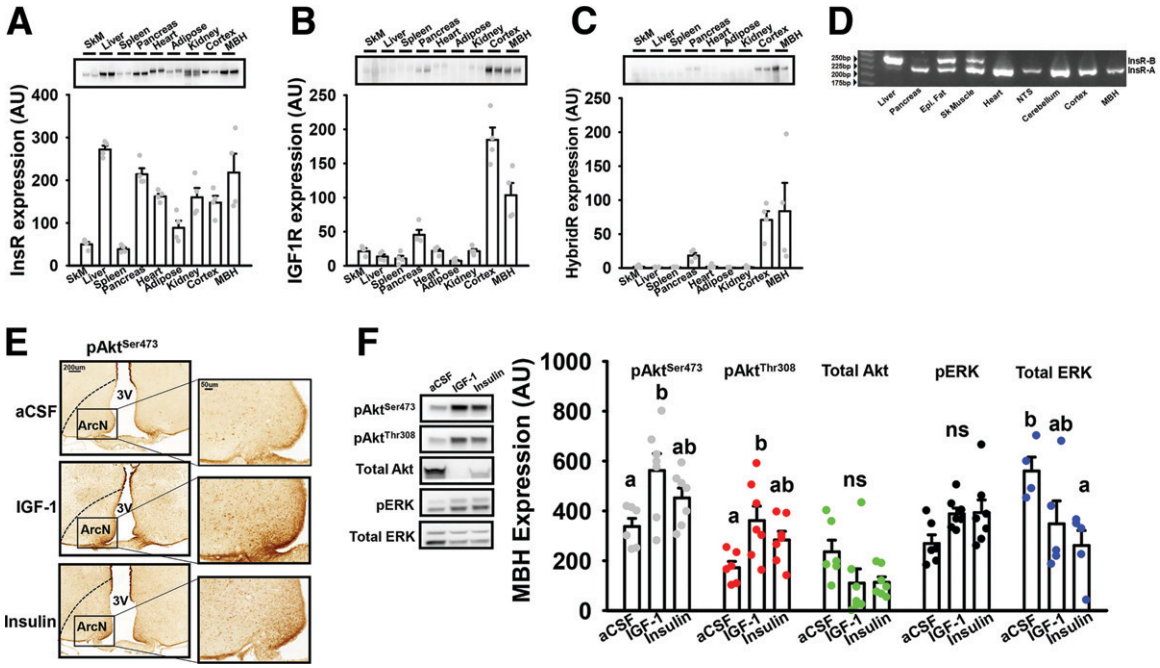

Figure 1—IGF-1Rs, InsRs, and HybridRs are abundantly expressed in the MBH. *A*: In rats, InsR was expressed in multiple tissues, with the greatest levels detected in liver, pancreas, and MBH ($n = 4$ per tissue). *B*: IGF-1R was highly enriched in the brain, including cortex and MBH, but less abundant in most peripheral tissues ($n = 4$ per tissue). *C*: Similar to IGF-1R, HybridRs were also highly expressed in the brain and modestly expressed in pancreas but nearly undetectable elsewhere ($n = 4$ per tissue). *D*: InsR-A gene expression was the main isoform detected in pancreas and brain, and InsR-B was the predominant isoform expressed in liver, whereas muscle and fat expressed both isoforms. *E* and *F*: ICV administration of either IGF-1 or insulin to young male rats leads to pAkt (Ser473) activation in the ArcN, as confirmed by immunostaining (taken at 10×; zoomed inset presented at 20×) and Western blotting in MBH enriched fractions ($n = 6$ aCSF, $n = 7$ IGF-1, $n = 7$ insulin). Bars graphs represent means ± SE, and circles indicate individual data points. Different letters denote a significant difference between groups, $P < 0.05$. AU, arbitrary units; bp, base pairs; Epi., epididymal; ns, not statistically significant; NTS, nucleus of the solitary tract; SkM, skeletal muscle.

downregulated total Erk content in MBH, as compared with controls ($P < 0.05$).

Selective Inhibition of Brain IGF-1Rs Prevents Suppression of HGP by Central Insulin or IGF-1

Prior to performing in vivo studies, we first aimed to confirm the specificity of the blocking reagents in vitro using two different neuronal cell lines, SH-SY5Y and mHypoA-NPY/GFP (Supplementary Fig. 1). Both cells lines were found to express InsRs and IGF-1Rs (Supplementary Fig. 1*A* and *D*). Moreover, as anticipated, pretreatment with IGF-1 mAb blunted the ability of IGF-1 to activate pAkt and pERK in SH-SY5Y cells and mHypoA-NPY/GFP cells (Supplementary Fig. 1*B* and *C*), while S961 tended to interfere with the ability of insulin to trigger pAkt and pERK in these same cells (Supplementary Fig. 1*E* and *F*). We next aimed to determine whether the ability of central IGF-1 to regulate HGP during hyperinsulinemic-glycemic clamps in rats is mediated via IGF-1Rs (Fig. 2*D*). To this end, animals were preemptively infused with ICV aCSF as vehicle, a selective IGF-1R mAb antagonist, or the InsR antagonist S961 15 min prior to chronic infusion of ICV vehicle, IGF-1, or insulin. As expected, the GIR needed to maintain euglycemia was increased with central infusion of insulin or IGF-1 (Fig. 2*E*) ($P < 0.001$), which was explained mainly by the suppression of HGP (Fig. 2*F*) by IGF-1 ($P < 0.001$) and insulin ($P < 0.05$), respectively, and a significant increase in R_d, as compared with aCSF controls (Fig. 2*G*). Preemptive infusion of IGF-1R mAb completely prevented the ability of IGF-1 to increase GIR or accentuate suppression of HGP and glucose uptake over controls, suggesting that that the central actions of IGF-1 are indeed mediated by its cognate receptor. However, IGF-1R mAb treatment not only abrogated the central effects of IGF-1 but also completely prevented the ability of central insulin to increase GIR (Fig. 2*E*) or suppress HGP (Fig. 2*F*). Moreover, ICV IGF-1R mAb tended to raise basal glucose, which was significant between ICV IGF-1 and ICV IGF-1+ICV mAb groups (Supplementary Fig. 2*A*) ($P < 0.05$).

To interfere with insulin signaling, we also administered S961, which alone had mild agonist effects on the GIR ($P = 0.09$) and HGP ($P = 0.10$), and S961 has previously been noted to have agonist activity on HybridRs at some doses (34). However, S961 resulted in the complete inability of central insulin to increase GIR, but unlike the IGF-1R mAb, S961 did not interfere with the ability of IGF-1 to increase GIR but did alter glucose fluxes such that

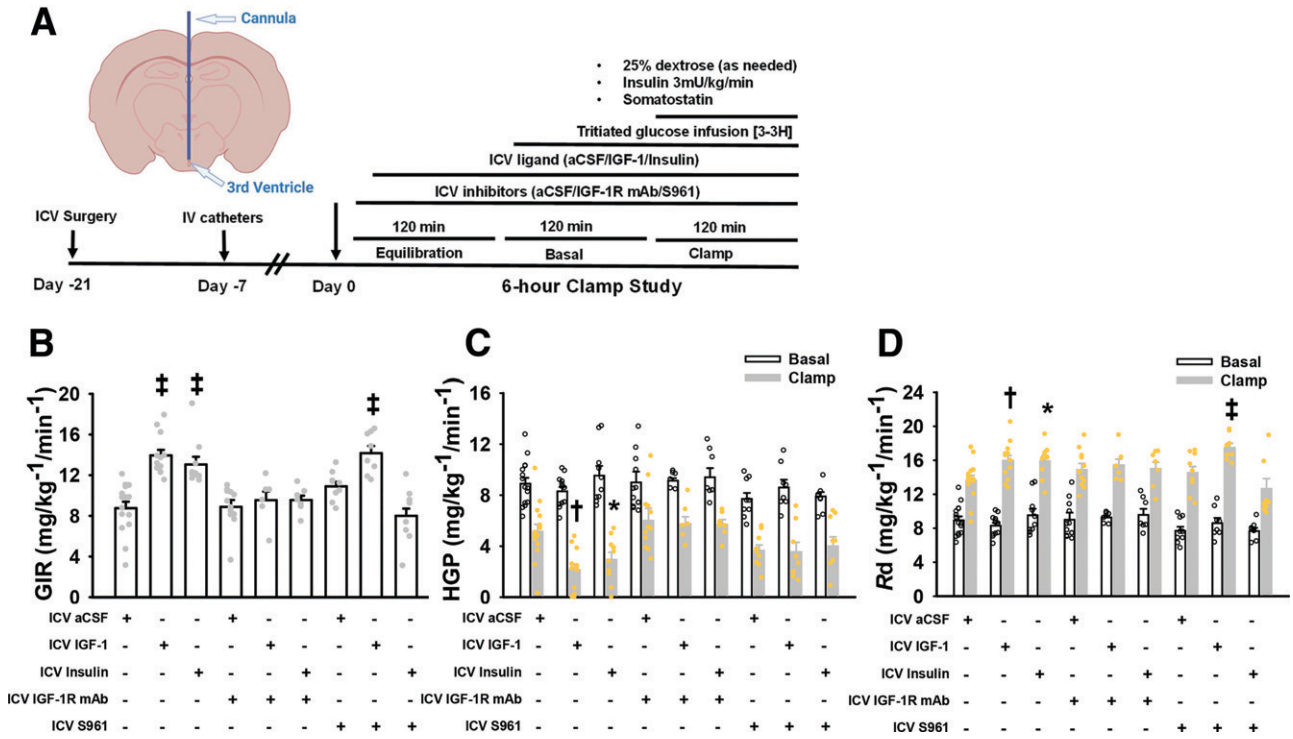

Figure 2—Selective inhibition of IGF-1R and InsR signaling reveals a critical role of central IGF-1Rs in the regulation of glucose metabolism: *A:* Experimental design of hyperinsulinemic-clamp studies in rats. Created with BioRender (biorender.com). *B–D*: GIR was increased with administration of either ICV insulin or IGF-1 in rats. However, with preemptive treatment with an IGF-1R inhibitor via ICV infusion, the ability of central IGF-1 or insulin to enhance GIR was abrogated, as was the ability of central insulin to suppress HGP. Likewise, S961 completely prevented the ability of ICV insulin to enhance GIR and suppress HGP, but did not interfere with the ability of ICV IGF-1to enhance GIR, though the effect was shifted to an increase in glucose disposal rather than suppression of HGP (aCSF controls $n = 15$, ICV IGF-1 $n = 12$, ICV insulin $n = 10$, ICV IGF-1R mAb only $n = 12$, ICV IGF-1+IGF-1R mAb $n = 6$, ICV insulin+IGF-1R mAb $n = 7$, ICV S961 only $n = 10$, ICV S961+IGF1 $n = 8$, ICV S961+insulin $n = 8$). Bar graphs indicate means ± SE, and circles indicate individual data points. *$P < 0.05$, †$P < 0.01$, ‡$P < 0.001$ vs. aCSF control after Dunnett post hoc adjustment.

central IGF-1 further increased glucose disposal ($P < 0.001$) rather than lowering HGP (Fig. 2*F* and *G*). Moreover, these effects occurred in the absence of differences in clamp glucose or insulin levels among groups (Supplementary Fig. 2). We further assessed expression of several metabolic genes in liver collected following clamp studies (Fig. 3*A–G*). Interestingly, ICV IGF-1R mAb and, to some extent, ICV S961 tended to increase liver expression of several gluconeogenic genes, which was significant for *Gck*, as compared with ICV IGF-1–infused animals (Fig. 3*B*) ($P < 0.05$). However, no significant effects were observed in estimated whole-body glycolysis or glycogen synthesis rates among groups (Fig. 3*H* and *I*). Meanwhile, liver *IL-6* expression was significantly greater in rats receiving ICV insulin that were preemptively treated with IGF-1R mAb, as compared with rats receiving either IGF-1R mAb or S961 alone (Fig. 3*E*), suggesting that this known effect of central nervous system (CNS) insulin was enhanced by selectively blocking IGF-1Rs. Taken together, these results suggest that IGF-1Rs may play a previously unappreciated role in mediating the effects of central insulin on whole-body glucose homeostasis.

Hyperinsulinemia Fails to Suppress Glucose Production in Mice Lacking IGF-1Rs in AgRP Neurons

Given that InsRs in AgRP neurons were previously demonstrated to be necessary for the central effects of insulin to suppress HGP, we next aimed to determine the potential role of IGF-1Rs in this neuronal population. We first set out to confirm the presence of IGF-1Rs in NPY/AgRP neurons. To this end, we collected cytoplasm from individual NPY/AgRP neurons in hypothalamic slices from reporter mice that express eGFP specifically in these cells. Amplified cDNA from individual NPY/AgRP cells showed that NPY/AgRP neurons express both InsR and IGF-1R (Fig. 4*A*), which we confirmed by sequencing the amplified products.

We next generated mice lacking IGF-1Rs specifically in AgRP neurons (referred to hereafter as KO mice) and examined effects on energy balance and glucose metabolism. KO animals appeared normal and did not show any obvious signs of growth or endocrine abnormalities, and IGF-1Rs appeared to be intact at other sites, including cortex and lung, suggesting that deletion was restricted to AgRP neurons (Supplementary Fig. 3*A* and *B*). Male KO

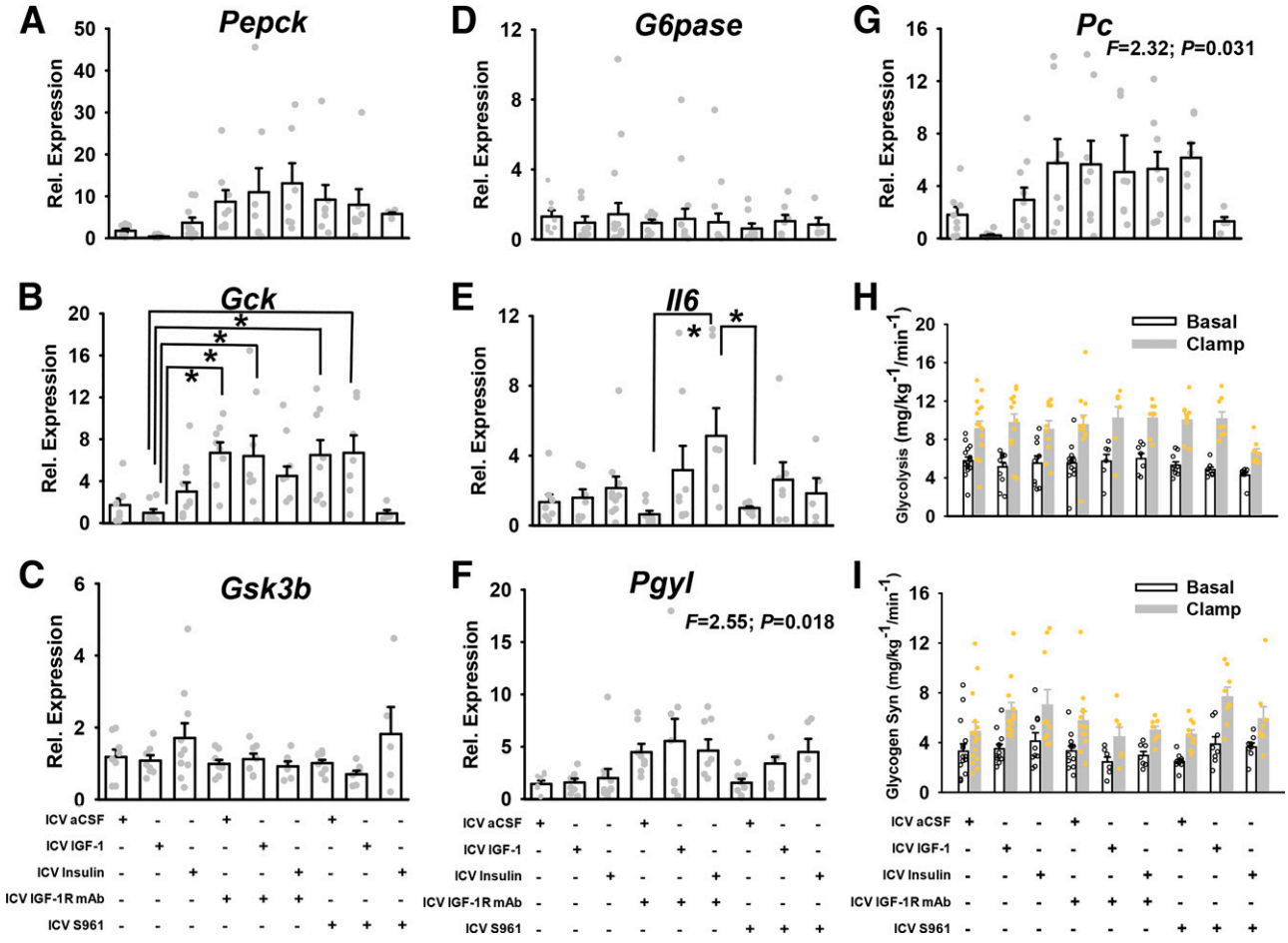

Figure 3—Expression of metabolic genes in rat liver following hyperinsulinemic-euglycemic clamps. *A–F*: We assessed expression of several metabolic genes in liver from rats collected immediately after a hyperinsulinemic-euglycemic clamp, including *Pepck*, *Gck*, *Gsk3b*, *G6pase*, *Il6*, *Pgyl*, and *Pc*. While ICV IGF-1R mAb and, to some extent, ICV S961 tended to increase liver expression of several gluconeogenic genes, there was no significant effect among groups for *Pepck*, *G6Pase*, *Gsk3b*, *Pc*, or *Pgyl*, but *Gck* was significantly increased in most groups receiving either ICV IGF-1R mAb or S961, as compared with ICV IGF-1 alone. Moreover, liver *IL-6* expression was significantly greater in rats receiving ICV insulin that were preemptively treated with IGF-1R mAb, as compared with rats receiving either IGF-1R mAb or S961 alone (aCSF controls $n = 8$, ICV IGF-1 $n = 8$, ICV insulin $n = 10$, ICV IGF-1R mAb only $n = 8$, ICV IGF-1+IGF-1R mAb $n = 7$, ICV insulin+IGF-1R mAb $n = 8$, ICV S961 only $n = 10$, ICV S961+IGF1 $n = 7$, ICV S961+insulin $n = 5$). *H* and *I*: However, no significant effects were observed in estimated whole-body glycolysis or glycogen synthesis (Syn) rates among groups during the clamp. Bar graphs indicate means ± SE, and dots indicate individual data points. *$P < 0.05$ after Tukey post hoc adjustment. Rel., relative.

mice did not show any differences in body weight (Fig. 4*B*) or food intake (Fig. 4*C*) up to 4 months of age, and there were not any differences in 4-h fasting insulin (Fig. 4*D*) compared with controls. Similarly, no differences in energy or glucose metabolism were observed in female KO mice (Supplementary Fig. 4*A–D*). Furthermore, GTTs (Fig. 4*E*) and ITTs (Fig. 4*F*) revealed no significant differences between groups for glucose or insulin tolerance, respectively, in males. However, when challenged with a PTT, male KO mice showed a significant increase in glucose levels over 2 h, suggesting a potential defect in hepatic gluconeogenesis compared with control mice (Fig. 4*G* and *H*) ($P < 0.05$).

To more definitively determine the impact of IGF-1Rs in AgRP neurons on glucose metabolism, we performed hyperinsulinemic-euglycemic clamps in control and KO mice (Fig. 5*A*). Plasma glucose and insulin levels were similar between groups during the clamp (Fig. 5*B* and *C*). However, consistent with PTT results, KO mice demonstrated an ∼30% reduction in the GIR (Fig. 5*D*) ($P < 0.05$) that was due mainly to an impaired ability to completely suppress HGP (Fig. 5*E*) ($P < 0.05$), without effects on R_d (Fig. 5*F*), compared with control mice.

Activation of Insulin Signaling in NPY/AgRP Neurons Is Dependent On the Presence of IGF-1Rs

To determine whether the physiologic consequences of lacking IGF-1Rs could be corroborated by signaling studies, we catheterized control and KO mice expressing the eGFP reporter in NPY/AgRP neurons and performed acute

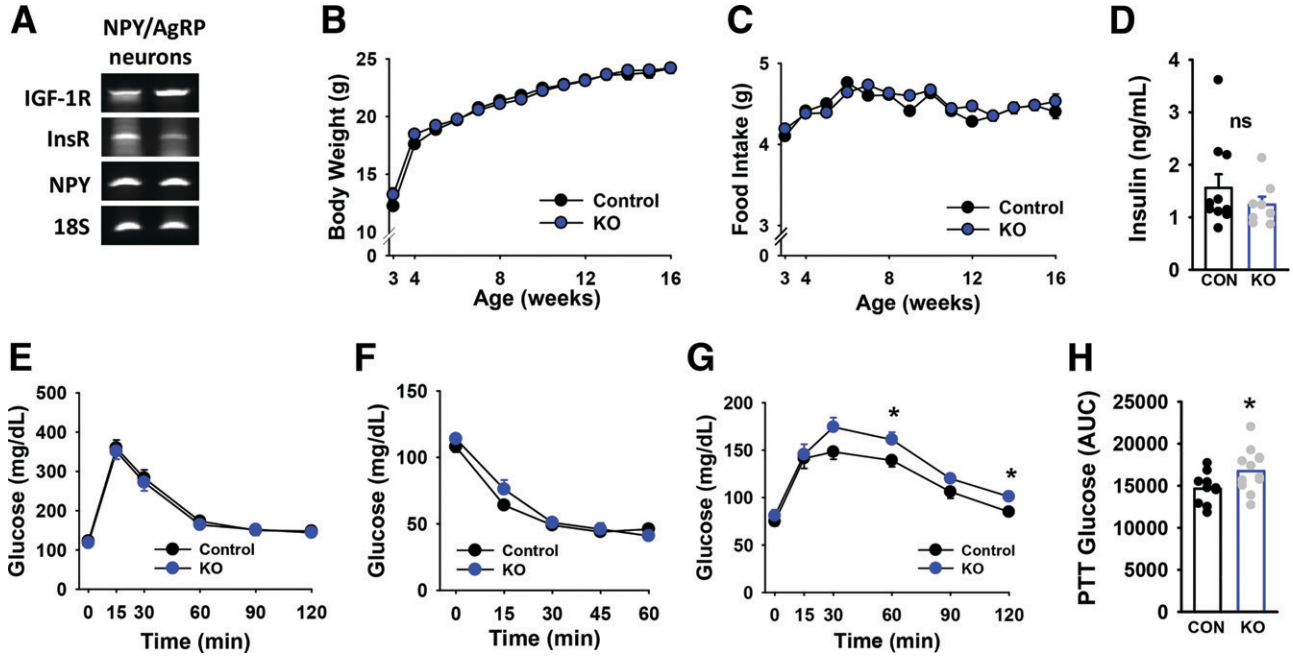

Figure 4—Metabolic phenotype of male mice lacking IGF-1Rs in AgRP neurons. *A*: Using single-cell quantitative PCR, we demonstrate that both IGF-1Rs and InsRs are expressed in all examined NPY/AgRP neurons ($n = 4$ neurons). *B–D*: Body weight, food intake ($n = 13$ controls [CON], $n = 12$ KO), and fasting insulin levels ($n = 11$ controls, $n = 8$ KO) were not significantly different in male KO animals compared with controls. *E* and *F*: Similarly, no differences were seen between groups during GTT or ITT ($n = 10$ controls, $n = 13$ KO). *G* and *H*: Nevertheless, KO animals showed increased glucose levels during a PTT, as compared with controls. Data are represented as means ± SE, and dot overlays indicate individual data points. *Significant difference between groups, $P < 0.05$. AUC, area under the curve; ns, not statistically significant.

intravenous infusions with saline or insulin. A peripheral insulin challenge was able to stimulate both pS6 (Fig. 6*A* and *B*) ($P < 0.05$) and PIP_3 (Fig. 6*C* and *D*) formation ($P < 0.05$) by more than twofold in NPY/AgRP neurons versus saline-injected controls. Likewise, while insulin-stimulated pS6 and PIP_3 levels were well visualized in surrounding hypothalamic cells of both control and KO mice, pS6 and PIP_3 in colocalized NPY/AgRP neurons were markedly attenuated in mice lacking IGF-1Rs in these cells (Fig. 6*A–D*). Thus, these data demonstrate an impaired ability of insulin to stimulate canonical downstream targets in AgRP neurons lacking IGF-1Rs, which supports relative insulin resistance observed in these animals under clamp conditions.

DISCUSSION

Several lines of evidence now support the notion that regulation of HGP by insulin is dependent on InsR signaling not only in hepatocytes, but also in extrahepatic tissues (1–8,35). Indeed, disruption of insulin signaling in the CNS has been shown to be sufficient to perturb glucose homeostasis at the level of the liver (2,3,8) as well as lipid metabolism in rodents (36–38). Previous studies have shown that interfering with CNS insulin signaling in the MBH (2,3,8) or dorsal vagal complex (7) using antisense, pharmacologic, or genetic strategies, respectively, is sufficient to impair suppression of HGP. However, the strongest evidence for a discrete extrahepatic cell population in the direct control of HGP involves AgRP neurons in the MBH (5,6,8). As a result, the ability of insulin to regulate HGP via the brain is often characterized by its ability to bind InsRs on AgRP neurons, thereby triggering downstream signaling, FOXO translocation, and neuronal hyperpolarization to drive this brain-liver circuit (39,40).

Similar to insulin, we have previously found that central administration of IGF-1 can suppress HGP (15) and is even more potent than central insulin at restoring peripheral insulin action in aged Sprague-Dawley rats (19). Therefore, we initially aimed to gain a better understanding as to how the effects of central IGF-1 on HGP are mediated, including the extent to which signaling was dependent on InsRs and/or IGF-1Rs. While many similarities exist between insulin and IGF-1 signaling, these pathways still serve to elicit distinct effects due to unique properties of the InsR and IGF-1R, cellular distribution, and the way in which ligand interacts with their respective receptor (17,18). While our results unequivocally demonstrate that central IGF-1 signaling requires its cognate receptor to regulate HGP, they unexpectedly show a previously unappreciated requirement for IGF-1Rs in the brain, and specifically at the level of AgRP neurons, in mediating the ability of insulin to suppress HGP. Könner

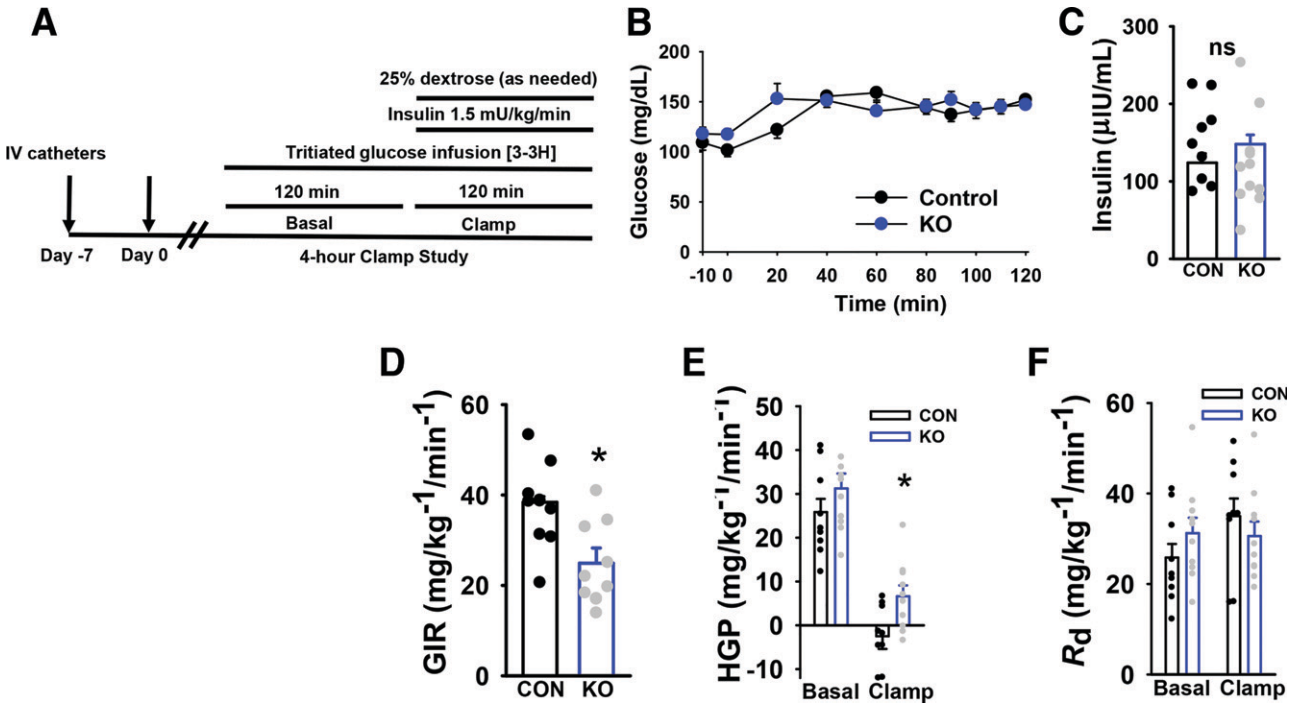

Figure 5—The ability of insulin to suppress HGP is impaired in mice lacking IGF-1Rs in AgRP neurons. *A*: To determine whether mice lacking IGF-1Rs in AgRP neurons have impaired regulation of HGP, we performed hyperinsulinemic-euglycemic clamps in mice. *B* and *C*: Animals were clamped under glucose and insulin levels that were similar between groups. *D*: Under hyperinsulinemia, KO mice had attenuated GIR. *E–G*: The reduction in GIR was due to an impaired ability to suppress HGP and was not due to differences in R_d compared with controls ($n = 10$ controls, $n = 10$ KO). Data are represented as means ± SE, and dots represent individual data points. *Significant difference between groups, $P < 0.05$. CON, control; ns, not statistically significant.

et al. (8) elegantly showed previously that InsR signaling in AgRP neurons was essential for suppression of HGP (8). However, given the complexity of clamp studies in rodents, it is difficult to speculate at this stage on the relative contribution of the IGF-1R versus InsR in AgRP neurons in disrupting central regulation of HGP across studies, though the relative degrees of suppression under hyperinsulinemia between control and KO animals in this study and that of Könner et al. (8) seem somewhat comparable. Moreover, the GIR did not appear to be compromised in $InsR^{\Delta AGRP}$ mice under clamp conditions (8), while mice in this study lacking IGF-1Rs in AgRP neurons demonstrated a marked 30% reduction in the GIR, demonstrating that these animals were more insulin resistant than controls.

Given the clear evidence that disrupting InsRs in the CNS is sufficient to prevent central regulation of HGP by insulin (2,8), how to reconcile the apparent requirement of IGF-1Rs in these effects is not yet clear, but there are a few potential explanations. One possibility involves a codependency of both InsRs and IGF-1Rs being present and active in these neurons in order to trigger a sufficient response to ligand binding via collateral signaling to instigate these neuronal effects. There is some precedent for this, as there are examples of IGF-1 dependency on InsRs, such as in the regulation of body temperature by the anterior hypothalamus (41), as well as the induction of more severe phenotypes on metabolism (42–45) and behavior (46) by removal of both InsRs and IGF-1Rs, thereby eliminating collateral signaling via either ligand on this pathway. On the other hand, loss of IGF-1Rs and HybridRs in osteoblasts or preadipocytes actually increases the sensitivity to insulin in these cells (47,48). These studies postulate that the mere presence of IGF-1Rs and HybridRs in these cell types might temper InsR signaling (47). It is also conceivable, though only speculative, that in removing IGF-1Rs, and hence the ability to form HybridRs, there is a greater ability for InsR homodimer formation in cells, thereby increasing insulin responses. However, it is unclear to what extent if any, removal of InsRs by past studies, or IGF-1Rs in the current investigation, altered abundance of the IGF-1R or InsR, respectively.

A related possibility involves signaling through a third receptor, HybridR. Indeed, deleting InsRs or IGF-1Rs, respectively, not only results in removal of the cognate receptor but also eliminates the ability to form HybridRs, which are heterotetramers of the α- and β-subunits of InsR and IGF-1R, respectively. The complexity of HybridR combinations is further increased by the presence of InsR-A (no exon 11) and InsR-B (49), with our data suggesting that the brain is composed mainly of the former

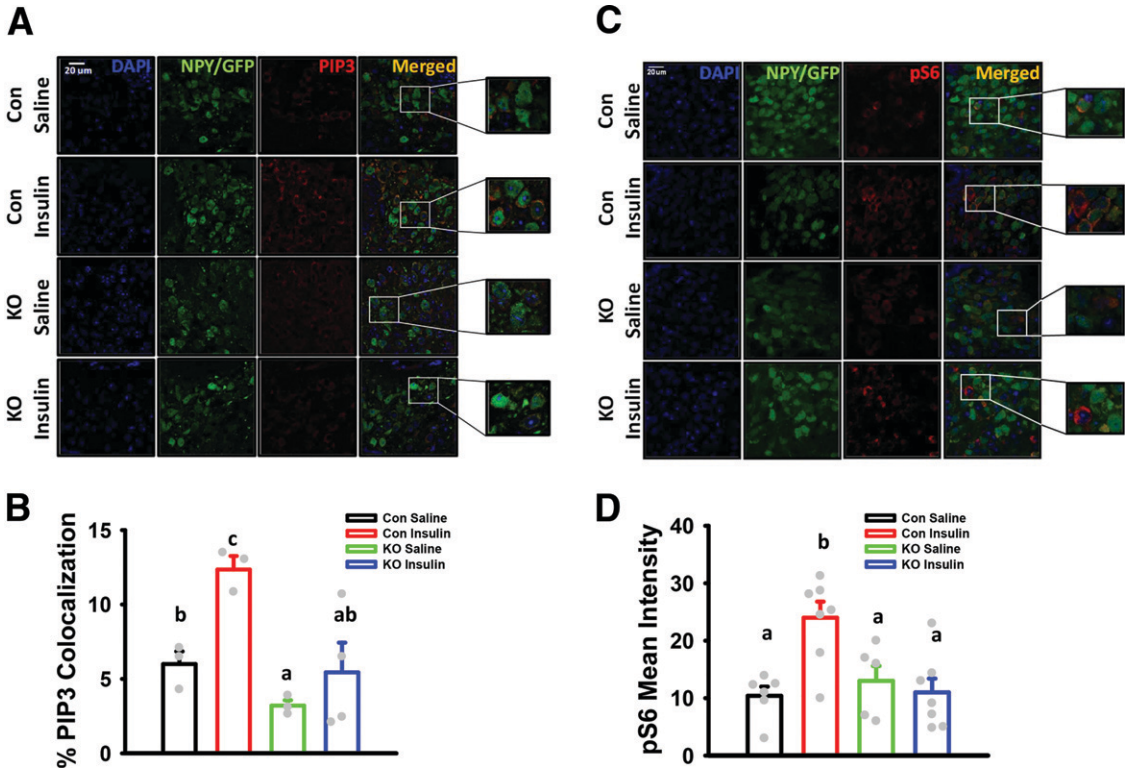

Figure 6—Absence of IGF-1Rs in NPY/AgRP neurons attenuates the ability of systemic insulin to trigger metabolic signaling pathways in these cells. *A* and *B*: Administering an IV insulin challenge (0.2 units/min over 5 min; 1 unit total dose), but not saline, results in increased pS6 mean fluorescence intensity within NPY/AgRP cells in control animals, but insulin was unable to activate pS6 in KO mice ($n = 6$ saline control [Con], $n = 7$ insulin control, $n = 5$ saline KO, $n = 7$ insulin KO). *C* and *D*: Deconvoluted representative images are shown for PIP_3 fluorescence. Similar to pS6, administration of IV insulin resulted in a significant increase in PIP_3% colocalization with NPY/AgRP neurons in control mice. Saline-infused KO mice had a slight, but significant, reduction in PIP_3 levels in AgRP/NPY neurons, as compared with saline Control mice, while similar to pS6, insulin was unable to activate PIP_3 in NPY/AgRP neurons from KO mice ($n = 3$ saline control, $n = 3$ insulin control, $n = 3$ saline KO, $n = 4$ insulin KO). Bar graphs represent means ± SE, and dot overlays indicate individual data points. Different letters denote significant difference between groups after Tukey honestly significant difference adjustment, $P \leq 0.05$.

isoform, and as a result, InsR-A/IGF-1R Hybrids should comprise the vast majority of these receptors in MBH and elsewhere in the CNS.

While the stoichiometry of HybridRs in tissues remains somewhat controversial, it is generally believed that formation of HybridRs occurs stochastically in the endoplasmic reticulum in any cell type that expresses InsR and IGF-1Rs, prior to reaching the cell membrane (50–52). Radioligand studies have suggested that HybridRs comprise nearly half of all InsRs and IGF-1Rs in some tissues. Interestingly, our data also show that IGF-1Rs and HybridRs are particularly enriched in brain tissue, including MBH, as compared with peripheral tissues, at least as a function of total protein load (52). Interestingly, a recent study showed that InsRs and IGF-1Rs are present in all of the major cell types in the brain and also showed that HybridRs are highly expressed in neurons, microglia, and astrocytes, with much less abundance in endothelial cells and oligodendrocytes (53). While we did not measure the presence of HybridRs in individual NPY/AgRP neurons per se, we did confirm that both IGF-1Rs and InsRs are expressed in the same NPY/AgRP neurons at the single-cell level, thereby supporting the likelihood that these heterodimers could form under stochastic processes in these cells as they have been shown to do in other neurons (53).

Presence and function of HybridRs in normal physiology have been understudied and are still debatable (51), though the general consensus is that they function as receptor tyrosine kinases, albeit more as IGF-1Rs, given their relatively lower affinity for insulin than IGF-1 (54). Progress in deciphering the role of these receptors has been particularly difficult because technologies that effectively allow for the specific recognition of the HybridR, without targeting either homodimer also present in the same cells or tissues, have not been developed. Indeed, our pharmacologic approach involved an IGF-1R mAb that selectively antagonizes both IGF-1Rs and HybridRs (22), while our genetic approach of deleting IGF-1Rs also presumably eliminated HybridRs in AgRP neurons and was sufficient to diminish the ability of central or peripheral insulin to regulate HGP or activate canonical signaling in NPY/AgRP neurons.

Meanwhile, S961 has been shown to have antagonist effects on both InsRs and HybridRs (23), which might explain the inability of either insulin or IGF-1 to significantly suppress HGP in the presence of S961 or IGF-1R mAb, as compared with controls, which was achieved with either ligand alone. Future studies that compare the effects of antibodies capable of blocking both the cognate receptor and HybridR versus antagonists against only the cognate receptor could be leveraged to better tease apart the isolated effects of HybridRs in normal physiology.

In summary, our results show that a pharmacologic approach to specifically target IGF-1Rs (and HybridRs), but not InsRs in the brain, was sufficient to interfere with not only IGF-1 but also central insulin in whole-body insulin action, particularly at the level of the liver. Furthermore, the inability of systemic hyperinsulinemia to trigger downstream signaling in NPY/AgRP neurons or completely suppress HGP in mice lacking IGF-1Rs in these neurons suggests that this mechanism might involve more than simply insulin triggering InsRs on AgRP neurons to exert its effects. Instead, these data suggest that IGF-1Rs as well as potentially HybridRs might be of importance in mediating the central effects of insulin on glucose metabolism, particularly in liver. Given that deletion of HybridRs is common to both InsR and IGF-1R KO models, the collective activation of these heterotetramers in AgRP neurons by insulin may be critical for sufficient triggering of downstream effects in these neurons to effectively suppress HGP in normal physiology. Furthermore, results of this study could have potential translational implications regarding strategies that have been leveraged to target insulin to the brain via the intranasal route. Indeed, the potential importance of IGF-1Rs– and HybridRs-mediated signaling in these CNS effects suggests that IGF-1 and related analogs should also be explored and leveraged as a potential therapeutic option for treating metabolic disease.

Acknowledgments. The authors thank Drs. Young-Hwan Jo and Gary Schwartz, both at the Albert Einstein College of Medicine and Fleischer Institute for Diabetes & Metabolism, for valuable input. The authors also acknowledge Vera DesMarais and Hillary Guzik for expert advice/assistance in microscopy and software analysis. The authors also acknowledge Zunju Hu, Hongqian Liang, and Ardijana Novaj for technical assistance.

Funding. This work was supported by National Institutes of Health grant R00 AG037574 and Einstein Startup Funds to D.M.H. D.M.H. was also a recipient of an American Federation for Aging Research junior faculty award while conducting this work. This study was also supported by National Institutes of Health grant R37 AG018381 and the Albert Einstein College of Medicine Nathan Shock Center (P30 AG038072) to N.B. and the Einstein–Mount Sinai Diabetes Research Center (P30 DK020541). The authors also acknowledge support from the National Cancer Institute–supported Albert Einstein Cancer Center (P30 CA013330). Einstein Analytical Imaging Core use was supported by National Institutes of Health Shared Instrument Grant (SIG) Program awards (1S10OD019961-01 and 1S10OD023591-01). The authors thank Dr. Lauge Schäffer (Novo Nordisk) for providing S961 material and Amgen Inc. for supplying IGF-1R mAb.

Duality of Interest. No potential conflicts of interest relevant to this article were reported.

Author Contributions. P.J.B., N.B., and D.M.H. conceived the initial study, and P.J.B. provided advisement on experimental tools. G.F.Q., K.M., and D.M.H. designed the experiments. G.F.Q., K.M., and D.M.H. performed the experiments. G.F.Q., K.M., and D.M.H. analyzed and interpreted the data and wrote the manuscript, and P.J.B. and N.B. provided feedback on the manuscript. D.M.H. is the guarantor of this work and, as such, had full access to all the data in the study and takes responsibility for the integrity of the data and the accuracy of the data analysis.

References

1. Titchenell PM, Chu Q, Monks BR, Birnbaum MJ. Hepatic insulin signalling is dispensable for suppression of glucose output by insulin in vivo. Nat Commun 2015;6:7078

2. Obici S, Zhang BB, Karkanias G, Rossetti L. Hypothalamic insulin signaling is required for inhibition of glucose production. Nat Med 2002;8:1376–1382

3. Obici S, Feng Z, Karkanias G, Baskin DG, Rossetti L. Decreasing hypothalamic insulin receptors causes hyperphagia and insulin resistance in rats. Nat Neurosci 2002;5:566–572

4. Okamoto H, Obici S, Accili D, Rossetti L. Restoration of liver insulin signaling in Insr knockout mice fails to normalize hepatic insulin action. J Clin Invest 2005;115:1314–1322

5. Ren H, Cook JR, Kon N, Accili D. Gpr17 in AgRP neurons regulates feeding and sensitivity to insulin and leptin. Diabetes 2015;64:3670–3679

6. Lin HV, Plum L, Ono H, et al. Divergent regulation of energy expenditure and hepatic glucose production by insulin receptor in agouti-related protein and POMC neurons. Diabetes 2010;59:337–346

7. Filippi BM, Yang CS, Tang C, Lam TK. Insulin activates Erk1/2 signaling in the dorsal vagal complex to inhibit glucose production. Cell Metab 2012;16:500–510

8. Könner AC, Janoschek R, Plum L, et al. Insulin action in AgRP-expressing neurons is required for suppression of hepatic glucose production. Cell Metab 2007;5:438–449

9. Plum L, Belgardt BF, Brüning JC. Central insulin action in energy and glucose homeostasis. J Clin Invest 2006;116:1761–1766

10. Paranjape SA, Chan O, Zhu W, et al. Chronic reduction of insulin receptors in the ventromedial hypothalamus produces glucose intolerance and islet dysfunction in the absence of weight gain. Am J Physiol Endocrinol Metab 2011;301:E978–E983

11. Liu JP, Baker J, Perkins AS, Robertson EJ, Efstratiadis A. Mice carrying null mutations of the genes encoding insulin-like growth factor I (Igf-1) and type 1 IGF receptor (Igf1r). Cell 1993;75:59–72

12. Aneke-Nash CS, Parrinello CM, Rajpathak SN, et al. Changes in insulin-like growth factor-I and its binding proteins are associated with diabetes mellitus in older adults. J Am Geriatr Soc 2015;63:902–909

13. Rajpathak SN, He M, Sun Q, et al. Insulin-like growth factor axis and risk of type 2 diabetes in women. Diabetes 2012;61:2248–2254

14. Sandhu MS, Heald AH, Gibson JM, Cruickshank JK, Dunger DB, Wareham NJ. Circulating concentrations of insulin-like growth factor-I and development of glucose intolerance: a prospective observational study. Lancet 2002;359:1740–1745

15. Muzumdar RH, Ma X, Fishman S, et al. Central and opposing effects of IGF-I and IGF-binding protein-3 on systemic insulin action. Diabetes 2006;55:2788–2796

16. De Meyts P, Whittaker J. Structural biology of insulin and IGF1 receptors: implications for drug design. Nat Rev Drug Discov 2002;1:769–783

17. Entingh-Pearsall A, Kahn CR. Differential roles of the insulin and insulin-like growth factor-I (IGF-I) receptors in response to insulin and IGF-I. J Biol Chem 2016;291:22339–22340

18. Rabiee A, Krüger M, Ardenkjær-Larsen J, Kahn CR, Emanuelli B. Distinct signalling properties of insulin receptor substrate (IRS)-1 and IRS-2 in mediating insulin/IGF-1 action. Cell Signal 2018;47:1–15
19. Huffman DM, Farias Quipildor G, Mao K, et al. Central insulin-like growth factor-1 (IGF-1) restores whole-body insulin action in a model of age-related insulin resistance and IGF-1 decline. Aging Cell 2016;15:181–186
20. Muzumdar RH, Huffman DM, Atzmon G, et al. Humanin: a novel central regulator of peripheral insulin action. PLoS One 2009;4:e6334
21. Einstein FH, Fishman S, Bauman J, et al. Enhanced activation of a "nutrient-sensing" pathway with age contributes to insulin resistance. FASEB J 2008;22:3450–3457
22. Calzone FJ, Cajulis E, Chung YA, et al. Epitope-specific mechanisms of IGF1R inhibition by ganitumab. PLoS One 2013;8:e55135
23. Schäffer L, Brand CL, Hansen BF, et al. A novel high-affinity peptide antagonist to the insulin receptor. Biochem Biophys Res Commun 2008;376: 380–383
24. Mao K, Quipildor GF, Tabrizian T, et al. Late-life targeting of the IGF-1 receptor improves healthspan and lifespan in female mice. Nat Commun 2018;9:2394
25. Huffman DM, Augenlicht LH, Zhang X, et al. Abdominal obesity, independent from caloric intake, accounts for the development of intestinal tumors in Apc(1638N/+) female mice. Cancer Prev Res (Phila) 2013;6:177–187
26. Calabuig-Navarro V, Yamauchi J, Lee S, et al. Forkhead Box O6 (FoxO6) depletion attenuates hepatic gluconeogenesis and protects against fat-induced glucose disorder in mice. J Biol Chem 2015;290:15581–15594
27. Ayala JE, Bracy DP, Malabanan C, et al. Hyperinsulinemic-euglycemic clamps in conscious, unrestrained mice. J Vis Exp 2011;57:3188
28. McGuinness OP, Ayala JE, Laughlin MR, Wasserman DH. NIH experiment in centralized mouse phenotyping: the Vanderbilt experience and recommendations for evaluating glucose homeostasis in the mouse. Am J Physiol Endocrinol Metab 2009;297:E849–E855
29. Einstein FH, Huffman DM, Fishman S, et al. Aging per se increases the susceptibility to free fatty acid-induced insulin resistance. J Gerontol A Biol Sci Med Sci 2010;65:800–808
30. Serrano R, Villar M, Martínez C, Carrascosa JM, Gallardo N, Andrés A. Differential gene expression of insulin receptor isoforms A and B and insulin receptor substrates 1, 2 and 3 in rat tissues: modulation by aging and differentiation in rat adipose tissue. J Mol Endocrinol 2005;34:153–161
31. Walters RO, Arias E, Diaz A, et al. Sarcosine is uniquely modulated by aging and dietary restriction in rodents and humans. Cell Rep 2018;25:663–676.e6
32. Jeong JH, Woo YJ, Chua S Jr, Jo YH. Single-cell gene expression analysis of cholinergic neurons in the arcuate nucleus of the hypothalamus. PLoS One 2016;11:e0162839
33. Su Y, Lam TK, He W, et al. Hypothalamic leucine metabolism regulates liver glucose production. Diabetes 2012;61:85–93
34. Knudsen L, Hansen BF, Jensen P, et al. Agonism and antagonism at the insulin receptor. PLoS One 2012;7:e51972
35. Scherer T, Lindtner C, O'Hare J, et al. Insulin regulates hepatic triglyceride secretion and lipid content via signaling in the brain. Diabetes 2016;65:1511–1520
36. Lam TK, Gutierrez-Juarez R, Pocai A, et al. Brain glucose metabolism controls the hepatic secretion of triglyceride-rich lipoproteins. Nat Med 2007;13:171–180
37. Brüning JC, Gautam D, Burks DJ, et al. Role of brain insulin receptor in control of body weight and reproduction. Science 2000;289:2122–2125
38. Shin AC, Filatova N, Lindtner C, et al. Insulin receptor signaling in POMC, but not AgRP, neurons controls adipose tissue insulin action. Diabetes 2017;66:1560–1571
39. Kitamura T, Feng Y, Kitamura YI, et al. Forkhead protein FoxO1 mediates Agrp-dependent effects of leptin on food intake. Nat Med 2006;12:534–540
40. Belgardt BF, Okamura T, Brüning JC. Hormone and glucose signalling in POMC and AgRP neurons. J Physiol 2009;587:5305–5314
41. Sanchez-Alavez M, Osborn O, Tabarean IV, et al. Insulin-like growth factor 1-mediated hyperthermia involves anterior hypothalamic insulin receptors. J Biol Chem 2011;286:14983–14990
42. Softic S, Boucher J, Solheim MH, et al. Lipodystrophy due to adipose tissue–specific insulin receptor knockout results in progressive NAFLD. Diabetes 2016;65:2187–2200
43. O'Neill BT, Lee KY, Klaus K, et al. Insulin and IGF-1 receptors regulate FoxO-mediated signaling in muscle proteostasis. J Clin Invest 2016;126: 3433–3446
44. Boucher J, Softic S, El Ouaamari A, et al. Differential roles of insulin and IGF-1 receptors in adipose tissue development and function. Diabetes 2016;65:2201–2213
45. Boucher J, Mori MA, Lee KY, et al. Impaired thermogenesis and adipose tissue development in mice with fat-specific disruption of insulin and IGF-1 signalling. Nat Commun 2012;3:902
46. Soto M, Cai W, Konishi M, Kahn CR. Insulin signaling in the hippocampus and amygdala regulates metabolism and neurobehavior. Proc Natl Acad Sci U S A 2019;116:6379–6384
47. Fulzele K, DiGirolamo DJ, Liu Z, Xu J, Messina JL, Clemens TL. Disruption of the insulin-like growth factor type 1 receptor in osteoblasts enhances insulin signaling and action. J Biol Chem 2007;282:25649–25658
48. Entingh-Pearsall A, Kahn CR. Differential roles of the insulin and insulin-like growth factor-I (IGF-I) receptors in response to insulin and IGF-I. J Biol Chem 2004;279:38016–38024
49. Moller DE, Yokota A, Caro JF, Flier JS. Tissue-specific expression of two alternatively spliced insulin receptor mRNAs in man. Mol Endocrinol 1989;3: 1263–1269
50. Pandini G, Vigneri R, Costantino A, et al. Insulin and insulin-like growth factor-I (IGF-I) receptor overexpression in breast cancers leads to insulin/IGF-I hybrid receptor overexpression: evidence for a second mechanism of IGF-I signaling. Clin Cancer Res 1999;5:1935–1944
51. Belfiore A, Frasca F, Pandini G, Sciacca L, Vigneri R. Insulin receptor isoforms and insulin receptor/insulin-like growth factor receptor hybrids in physiology and disease. Endocr Rev 2009;30:586–623
52. Bailyes EM, Navé BT, Soos MA, Orr SR, Hayward AC, Siddle K. Insulin receptor/IGF-I receptor hybrids are widely distributed in mammalian tissues: quantification of individual receptor species by selective immunoprecipitation and immunoblotting. Biochem J 1997;327:209–215
53. Martinez-Rachadell L, Aguilera A, Perez-Domper P, Pignatelli J, Fernandez AM, Torres-Aleman I. Cell-specific expression of insulin/insulin-like growth factor-I receptor hybrids in the mouse brain. Growth Horm IGF Res 2019;45:25–30
54. Slaaby R. Specific insulin/IGF1 hybrid receptor activation assay reveals IGF1 as a more potent ligand than insulin. Sci Rep 2015;5:7911